materials

Article

Theoretical Nanoarchitectonics of GaN Nanowires for Ultraviolet Irradiation-Dependent Electromechanical Properties

Kun Yang [1], Guoshuai Qin [2,*], Lei Wang [3], Minghao Zhao [1,4,5] and Chunsheng Lu [6,*]

1 School of Mechanics and Safety Engineering, Zhengzhou University, Zhengzhou 450001, China
2 School of Electromechanical Engineering, Henan University of Technology, Zhengzhou 450001, China
3 Henan Institute of Metrology, Zhengzhou 450001, China
4 School of Mechanical Engineering, Zhengzhou University, Zhengzhou 450001, China
5 Henan Key Engineering Laboratory for Anti-Fatigue Manufacturing Technology, Zhengzhou University, Zhengzhou 450001, China
6 School of Civil and Mechanical Engineering, Curtin University, Perth, WA 6845, Australia
* Correspondence: gsqin@haut.edu.cn (G.Q.); c.lu@curtin.edu.au (C.L.)

Abstract: In this paper, we propose a one-dimensional model that combines photoelectricity, piezoelectricity, and photothermal effects. The influence of ultraviolet light on the electromechanical coupling properties of GaN nanowires is investigated. It is shown that, since the ultraviolet photon energy is larger than the forbidden gap of GaN, the physical fields in a GaN nanowire are sensitive to ultraviolet. The light-induced polarization can change the magnitude and direction of a piezoelectric polarization field caused by a mechanical load. Moreover, a large number of photogenerated carriers under photoexcitation enhance the current density, whilst they shield the Schottky barrier and reduce rectifying characteristics. This provides a new theoretical nanoarchitectonics approach for the contactless performance regulation of nano-GaN devices such as photoelectric sensors and ultraviolet detectors, which can further release their great application potential.

Keywords: ultraviolet photoexcitation; electromechanical coupling; photoconductive effects; photothermal effect; GaN nanowires

check for updates

Citation: Yang, K.; Qin, G.; Wang, L.; Zhao, M.; Lu, C. Theoretical Nanoarchitectonics of GaN Nanowires for Ultraviolet Irradiation-Dependent Electromechanical Properties. *Materials* **2023**, *16*, 1080. https://doi.org/10.3390/ma16031080

Academic Editor: Dominique de Caro

Received: 23 December 2022
Revised: 21 January 2023
Accepted: 23 January 2023
Published: 26 January 2023

1. Introduction

As a direct wide band gap semiconductor material, GaN exhibits high-power density, superior electrical and thermal conductivities, strong radiation resistance, and high breakdown voltage [1]. Owing to the size effect, GaN nanostructures exhibit a smaller Young's modulus and a higher quality factor, which makes them have obvious advantages in the application of nano-mechanical systems [2,3]. In addition, because of the piezoelectric and semiconductive properties, piezoelectric potential generated in a crystal can effectively regulate the carrier transport capacity of an interface/unction region under mechanical loading [4,5]. Such a unique synergistic effect makes the piezoelectric potential produce a similar "gate circuit", and hence, many novel modern electromechanical coupling devices have been developed, such as piezoelectric charge-coupled devices [6–8] and energy conversion supplies [9–13]. Inevitably, there is an urgent need for the active regulation of device performance.

GaN is a natural optoelectronic material. Due to the fact that the ultraviolet photon energy is larger than the forbidden gap of GaN (the energy band difference between conduction and valence bands [14]), the physical fields in a GaN nanowire are sensitive to ultraviolet. Irradiation can stimulate the generation, separation, transport, and recombination of carriers in GaN [15]. The available studies have mainly focused on regulating the electrical transport characteristics of piezoelectric semiconductors (PSCs) under mechanical loads [16] and doping [17]. There are few reports on regulating their electromechanical properties by means of light excitation [18–21]. For example, based on the photoelectric experiment of ZnO nanowires, Wang and Zhang found that ultraviolet light can weaken Schottky's rectification characteristics [22–24]. To the best of our knowledge, however, it is still a lack of quantitative analysis from the theoretical and numerical aspects. In practical applications, however, a device is inevitably affected by light irradiation, which can deteriorate the electrical properties of GaN materials through the generation-recombination of carriers. That is, radiation causes a certain disturbance of electrical properties. Therefore, it is necessary to investigate the influence of light irradiation on the electromechanical properties of GaN structures. It is expected that a new approach can be developed for the performance regulation of GaN devices without doping.

In this paper, GaN nanowires under a combined photoexcitation and electrical load are comprehensively investigated by using both theoretical and numerical methods. The paper is organized as follows. In Section 2, a one-dimensional (1-D) thermo-piezoelectric theory is first proposed, including the photoconductive and photothermal effects. Then, in Section 3, the influence of ultraviolet irradiation is analyzed on the physical fields of GaN nanowires, and photoexcitation regulation of the electrical transport properties is discussed in an Ag-GaN Schottky junction. Finally, several main conclusions are summarized in Section 4.

2. Basic Equations for a GaN Nanowire under Light Irradiation

Uniform light irradiation can cause temperature rising in a semiconductor structure. According to the principle of heat balance [25], the change in temperature versus time yields

$$C_T \frac{d(T-T_p)}{dt} + G_T(T-T_0) = SI, \tag{1}$$

where C_T is the heat capacity, and G_T = H_g A_g represents the heat exchange coefficient, with the air thermal convection coefficient H_g = 4 W K^{-1} m^{-2} and A_g the contact area between the semiconductor and air [26]. T_p and T_0 are the initial and room temperatures, respectively. S denotes the illumination area, and I is the light intensity.

At the beginning of illumination, the amount of variation in temperature $\Delta T(0) = 0$. Solving Equation (1), the temperature change can be obtained as

$$\Delta T(t) = T - T_p = \Delta T_{\mathrm{opt}}(1 - e^{-t/\tau_\theta}), \tag{2}$$

where ΔT_{opt} = S I/G_T is the maximum change of temperature in a steady state, and τ_θ is the thermal time constant. Here, it is worth noting that, when the illumination time t $\gg\tau_\theta$, the temperature change ΔT (t) = ΔT_{opt} = S I/G_T.

The electron-hole pairs in a semiconductor can be excited when the photon energy is higher than the band gap width [22]. That is, GaN can be excited by ultraviolet light to produce non-equilibrium carriers. Under uniform illumination, the non-equilibrium carrier concentrations in a steady state are described as [13]

$$\begin{aligned} \Delta n_{\mathrm{opt}} &= \beta\alpha P_{\mathrm{opt}}\lambda / hce^{-\alpha d}\tau_n, \\ \Delta p_{\mathrm{opt}} &= \beta\alpha P_{\mathrm{opt}}\lambda / hce^{-\alpha d}\tau_p, \end{aligned} \tag{3}$$

where β is the internal quantum efficiency, representing the number of photocarrier pairs excited by each photon. α is the absorption coefficient, P_{opt} is the illumination intensity, λ is the wavelength, and h and c are the Planck constant and light velocity, respectively. d represents the incident depth, and τ_n and τ_p are the lifetimes of non-equilibrium electrons and holes, respectively.

As illustrated in Figure 1, let us assume that photoexcited carriers gradually decay with the transmission depth of incident light. In the case of a 1-D nanowire with a radius of r, the average concentration of photo-generated carriers on its cross-section can be expressed as

$$\begin{aligned} \Delta\overline{n}_{\text{opt}} &= \Big(\iint\limits_{x^2+y^2\leq r^2} \Delta n_{\text{opt}} dxdy\Big)/\pi r^2, \\ \Delta\overline{p}_{\text{opt}} &= \Big(\iint\limits_{x^2+y^2\leq r^2} \Delta p_{\text{opt}} dxdy\Big)/\pi r^2. \end{aligned} \tag{4}$$

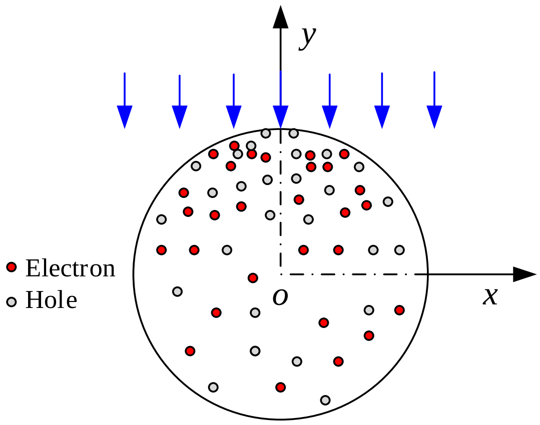

Figure 1. A schematic attenuation diagram of photoexcited carriers with the transmission depth under incident light.

Taking a 1-D GaN nanorod with a length of 2L as an example (see Figure 2), the c-axis is along the z-direction, with a uniform beam of ultraviolet light vertically irradiated on the upper surface. Its physical and mechanical behaviors are governed by the motion equation, electrostatics Gauss's law, and the current continuity equation [27–30], that is

$$\begin{aligned} \frac{\partial \sigma_{zz}}{\partial z} &= 0, \\ \frac{\partial D_z}{\partial z} &= q(p - n + N_D^+ - N_A^-), \\ \frac{\partial J_z^n}{\partial z} &= -qU_n, \\ \frac{\partial J_z^p}{\partial z} &= qU_p, \end{aligned} \tag{5}$$

where σ_{zz}, D_z, J_z^n, and J_z^p denote the stress tensor, electric displacement, electron concentration density, and hole current density. N_D^+ and N_D^- represent the ionization degrees of donor and acceptor impurities, respectively. q is the unit charge (1.602×10^{-19} C), and n and p are the electron and hole doping concentrations. U_n and U_p are the net recombination rates of free electrons and holes. Here, the generation and recombination of free electrons and holes are in a dynamic equilibrium state, that is, U_n and U_p are equal to 0.

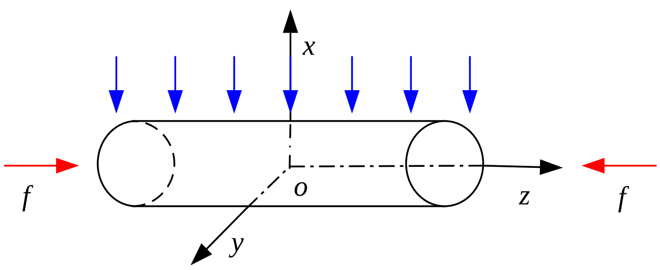

Figure 2. The physical model of ultraviolet irradiation on a GaN nanowire.

For a 1-D PSC with the polarization direction along the z-axis, the constitutive equation in Cartesian coordinates can be written as [31–34]

$$\begin{aligned}
\sigma_{zz} &= c_{33}\varepsilon_{zz} - e_{33}E_z - \lambda_{33}\Delta T_{\text{opt}}, \\
D_z &= e_{33}\varepsilon_{zz} + \kappa_{33}E_z + p_{33}\Delta T_{\text{opt}}, \\
J_z^n &= qn\mu_{33}^n E_z + qd_{33}^n \frac{\partial n}{\partial z}, \\
J_z^p &= qp\mu_{33}^p E_z - qd_{33}^p \frac{\partial p}{\partial z},
\end{aligned} \tag{6}$$

where ε_{zz} is the strain tensor, E_z is the electric field strength, c_{33} and e_{33} are the elastic and piezoelectric coefficients, κ_{33} is the dielectric constant, λ_{33} is the thermal expansion coefficient, and p_{33} is the pyroelectric coefficient. μ_{33}^n and μ_{33}^p are the mobilities of electrons and holes, and d_{33}^n and d_3^p represent the electron and hole diffusion constants. The mobility and diffusion of free carriers satisfy the Einstein relation [35], namely

$$\frac{\mu_{33}^n}{d_{33}^n} = \frac{\mu_{33}^p}{d_{33}^p} = \frac{q}{k_B T_0}. \tag{7}$$

where k_B is Boltzmann's constant and T_0 is the reference temperature. The strain ε_{zz} and the electric field E_z are related to the mechanical displacement u and the electric potential φ, respectively, that is

$$\begin{aligned}
\varepsilon_{zz} &= \frac{\partial u_z}{\partial z}, \\
E_z &= -\frac{\partial \varphi}{\partial z},
\end{aligned} \tag{8}$$

where u_z and φ are the mechanical displacement and electric potential, respectively.

Substituting Equation (6) into Equation (4), the governing equations are obtained by

$$\begin{aligned}
& c_{33}\frac{\partial^2 u}{\partial z^2} + e_{33}\frac{\partial^2 \varphi}{\partial z^2} - \lambda_{33}\frac{\partial(\Delta T_{\text{opt}})}{\partial z} = 0, \\
& e_{33}\frac{\partial^2 u}{\partial z^2} - \kappa_{33}\frac{\partial^2 \varphi}{\partial z^2} + p_{33}\frac{\partial(\Delta T_{\text{opt}})}{\partial z} = q(p - n + N_D^+ - N_A^-), \\
& -qn\mu_{33}^n \frac{\partial^2 \varphi}{\partial z^2} + qd_{33}^n \frac{\partial^2 n}{\partial z^2} = 0, \\
& -qp\mu_{33}^p \frac{\partial^2 \varphi}{\partial z^2} - qd_{33}^p \frac{\partial^2 p}{\partial z^2} = 0.
\end{aligned} \tag{9}$$

For an n-type GaN nanowire, the concentrations of acceptor and donor impurities are $N + D = 1 \times 10^{23}\ \text{m}^{-3}$ and $N_A^- = N_i^2/N + D$, where N_i is the concentration of intrinsic carriers. Other relevant material constants are listed in Table 1 [36–40]. Generally speaking, an analytic solution for such a nonlinear model is difficult to be obtained. Hence, to solve the photoexcitation physical problem, a numerical iterative method is adopted by using the PDE module in COMSOL Multiphysics software. Here it is worth noting that Guo and Yang obtained the approximate analytical solution of 1-D piezoelectric semiconductors by a perturbation method, and in comparison with the results from COMSOL, it can be applied to verify the reliability and accuracy of our calculation [41,42].

Table 1. Material constants used in the analysis of a GaN nanowire.

Property	Parameter	Value	Unit
Elastic constant	c_{33}	289.2	GPa
Piezoelectric constant	e_{33}	0.61	$C\ m^{-2}$
Dielectric constant	κ_{33}	9.39×10^{-11}	$F\ m^{-1}$
Hole mobility constant	μ_{33}^{p}	192	$cm^2\ V^{-1}\ s^{-1}$
Hole diffusion constant	d_{33}^{p}	5	$cm^2\ s^{-1}$
Electron mobility constant	μ_{33}^{n}	560	$cm^2\ V^{-1}\ s^{-1}$
Electron diffusion constant	d_{33}^{n}	25	$cm^2\ s^{-1}$
Thermal expansion coefficient	λ_{33}	1.69×10^{6}	$N\ m^{-2}\ K^{-1}$
Pyroelectric constant	p_{33}	-3.8×10^{-6}	$C\ m^{-2}\ K^{-1}$
Intrinsic carrier concentration	N_i	3.43×10^{-4}	m^{-3}
Photogenic electron lifetime	τ_n	1.67×10^{-5}	s
Photogenic hole lifetime	τ_p	1.67×10^{-5}	s
Optical absorption coefficient	α	1×10^{5}	cm^{-1}
Heat capacity at constant pressure	C_p	490	$J\ kg^{-1}\ K^{-1}$

3. Results and Discussion

Under the ultraviolet light with a wavelength of 350 nm and the mechanical conditions as illustrated in Figure 2, when there is no applied current across (in and out) the nanorod, the boundary conditions at the two ends can be written as

$$\begin{aligned} &\sigma_z(\pm L) = f, \\ &D_z(\pm L) = 0, \\ &J_z^n(\pm L) = 0, \\ &J_z^p(\pm L) = 0. \end{aligned} \tag{10}$$

Here, n and p satisfy the following electrical neutral conditions

$$\begin{aligned} &\int_{-l}^{l}\left(p - N_A^- - \Delta\overline{p}_{\text{opt}}\right)dz = 0, \\ &\int_{-l}^{l}\left(n - N_D^+ - \Delta\overline{n}_{\text{opt}}\right)dz = 0. \end{aligned} \tag{11}$$

At the position $z = 0$, the conditions of displacement and potential are

$$\begin{aligned} &u(0) = 0, \\ &\varphi(0) = 0. \end{aligned} \tag{12}$$

Due to the photoconductive effect, a large number of photogenerated carriers are produced with the increase in light intensity, which obviously enhances the concentration of free electrons and holes (see Figure 3a,b). In addition, ultraviolet light changes the distribution of carriers, especially at both ends. This is attributed to the synergy of piezoelectric and pyroelectric effects. That is, due to the photothermal effect, temperature increases under irradiation of light, which leads to the separation of positive and negative ions in GaN nanowires, resulting in pyroelectric charges. The polarity of pyroelectric polarization is opposite to that of piezoelectric polarization. With the increase of irradiation intensity, pyroelectric polarization becomes dominant, which changes the distribution of piezoelectric polarization charges (see Figure 4a). Similarly, because the direction of pyroelectric potential is opposite to the piezoelectric field generated by pressure, the piezoelectric potential is weakened and the comprehensive potential is even reversed (see Figure 4b,c). Consistent with the potential, the piezoelectric field decreases with the light intensity. When the light intensity reaches a certain value, the pyroelectric field plays a dominant role, and the comprehensive polarization field in GaN is opposite to that without ultraviolet light (see Figure 4d).

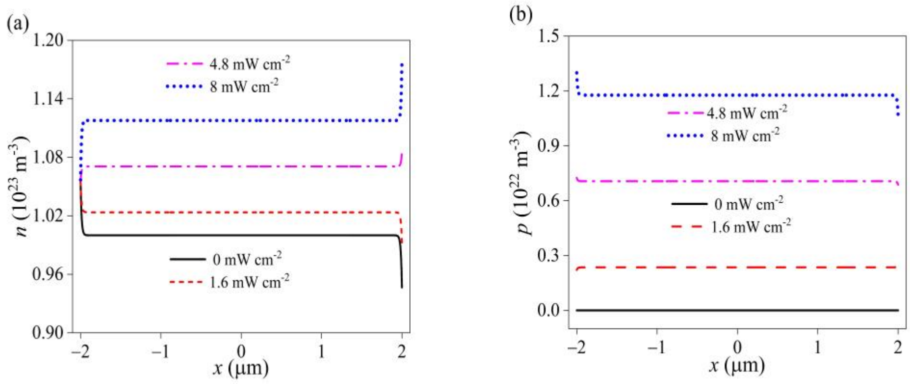

Figure 3. The carrier concentration distribution of (**a**) electron and (**b**) hole with different ultraviolet intensities under a compressive stress of −5 MPa.

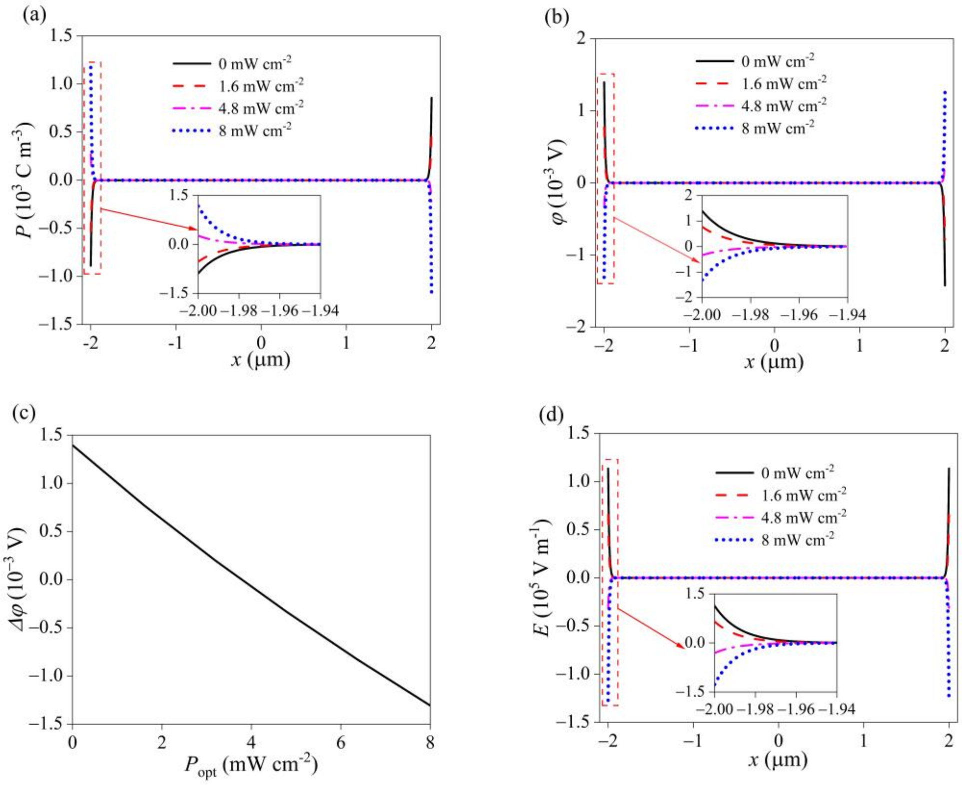

Figure 4. The physical field distributions of (**a**) the polarization charge density, (**b**) the electric potential, (**c**) the variation of the potential at the left end, and (**d**) the electric field under different ultraviolet intensities.

Let us take the Ag electrodes at both ends of a GaN nanowire as an example, which forms a double Schottky contact. As illustrated in Figure 2, the boundary conditions are

$$
\begin{aligned}
&\sigma_z(\pm L) = f, \\
&V(-L) = V_a + V_{bi} + V_b, \\
&V(L) = 0, \\
&J_z^n(\pm L) = -qv_{\mathrm{rec}}^n(n - n_m), \\
&J_z^p(\pm L) = qv_{\mathrm{rec}}^p(p - p_m),
\end{aligned}
\tag{13}
$$

where V_a is an applied bias voltage, V_{bi} is the built-in voltage, and V_b is the piezoelectric potential (i.e., the potential difference between the two ends caused by photoexcitation).

V_{rec}^{n} and V_{rec}^{p} denote the thermal recombination velocities of electrons and holes at the Schottky interface, respectively. n_m and p_m are the critical electron and hole concentrations, which can be represented as [43–47]

$$\begin{aligned} n_m &= N_c e^{-\Phi_B/k_B T}, \\ p_m &= n_i^2/n_m, \\ N_c &= 2\left(\frac{2\pi m_e k_B T}{h^2}\right)^{3/2}, \end{aligned} \tag{14}$$

where Φ_B is the GaN surface barrier when the electron energy is equal to the Fermi level, and T is the absolute temperature. $m_e = 1.82 \times 10^{-31}$ kg is the effective mass of conduction band electrons, and $N_c = 2.23 \times 10^{24}$ m^{-3} denotes the effective density of states of conduction bands. The built-in voltage, V_{bi} is defined by [43–45]

$$V_{bi} = \Phi_B - k_B T/q \ln(N_c/n_0), \tag{15}$$

and the Schottky contacts barrier height $q\Phi_B$ can be represented as [43,44]

$$q\Phi_B = q\Phi_M - q\chi, \tag{16}$$

which is the difference between the working function of silver ($q\Phi_M = 4.26$ eV) [23] and the electron affinity ($q\chi = 4.1$ eV) of GaN [38], leading to the potential difference, $\Phi_B = 0.16$ eV.

It is seen from Figure 5a that ultraviolet light can significantly change the *I-V* characteristics of a GaN Schottky junction. In the absence of light, there is an obvious rectification characteristic due to the Schottky barrier between GaN nanowires and Ag electrode. However, with the increase of ultraviolet power density, the Schottky contact rectification weakens and gradually shifts to the Ohmic contact. This is due to the pyroelectric polarization caused by the photothermal effect, which reduces the barrier height of a junction region. In addition, a large number of carriers generated by photoexcitation have a shielding effect on characteristics of the Schottky rectifier. When the photo-generated carriers increase to a particular concentration, the Schottky barrier is completely shielded, and the rectifying characteristics may be lost. That is, ultraviolet excitation can be applied to regulate the electrical transport behavior of GaN nanodevices.

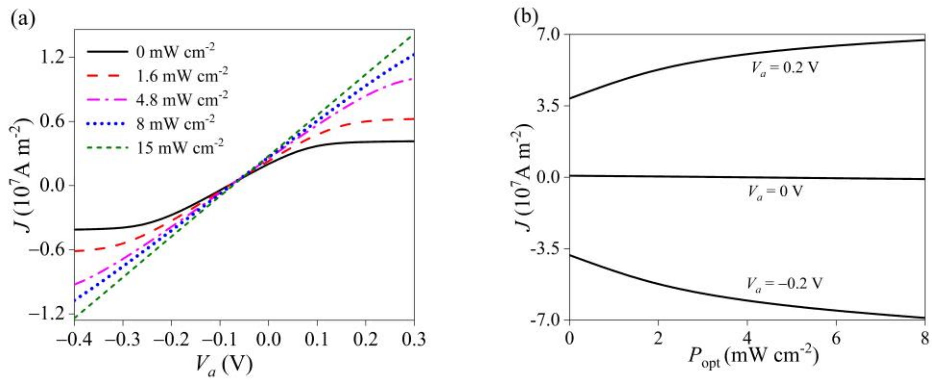

Figure 5. The characteristics of (**a**) *I–V* and (**b**) *I–*P_{opt} in a GaN nanowire under different ultraviolet intensities.

As shown in Figure 5b, the current increases gradually with the light intensity, regardless of a positive or a negative bias voltage. However, the increasing amplitude becomes smaller and tends to be saturated. That is mainly due to the photoconductivity effect, producing a large number of photo-generated carriers that increases the current density. In addition, the photothermal effect increases with the optical power density and produces a thermal electric field, which enhances the Schottky barrier and the shielding effect of the Schottky junction, and thus, the current is gradually saturated [47,48].

4. Conclusions

By using a 1-D PSC model, we have investigated the photoexcitation-dependent electrical behaviors in a GaN nanowire, which are conducive to applications in ultra-fast optics, nonlinear optics, photothermal detection, computational memory, and biocompatibility photodetectors. The main conclusions can be drawn as follows:

1. By incorporating the photoconductive and photothermal effects, a multi-field coupling model is proposed, which can consider photoexcitation nonequilibrium carriers in PSCs.
2. Due to the synergy of piezoelectricity, photoconductivity, and photoexcitation induced-pyroelectricity, the physical field distributions in a GaN nanowire are significantly affected by ultraviolet, including the polarization charge, potential, electric field, and carrier concentration.
3. Ultraviolet light can be applied to regulate the height of the Schottky barrier and even make the rectifying characteristics disappear. That is, the electrical correlation characteristics of a GaN Schottky junction device are highly sensitive to ultraviolet light. This provides a novel, non-contact method for tuning the electrical transport performance of a GaN Schottky junction device.
4. Finally, it is worth noting that, as a preliminary study and for simplification, the effects of ultraviolet excitation on the electromechanical properties of nanowires were only investigated by using theoretical and numerical methods in this work. Obviously, further experimental studies need to be done, such as the tests of the photoconductivity and photothermal effects, to verify the regulation of ultraviolet light on the electrical transmission properties and reveal the physical mechanism of such a complex and coupling problem.

Author Contributions: Conceptualization, G.Q. and C.L.; methodology, M.Z.; software, K.Y. and L.W.; validation, K.Y., G.Q.; formal analysis, K.Y.; investigation, C.L.; resources, K.Y.; data curation, K.Y. and L.W.; writing—original draft preparation, K.Y.; writing—review and editing, C. L.; visualization, G.Q.; supervision, M.Z.; project administration, K.Y. and L.W.; funding acquisition, G.Q. and C.L. All authors have read and agreed to the published version of the manuscript.

Funding: This research was funded by the National Natural Science Foundation of China, grant number Nos. 12002316 and 12272353.

Institutional Review Board Statement: Not applicable.

Informed Consent Statement: Not applicable.

Data Availability Statement: Data available on request due to restrictions e.g., privacy or ethical. The data presented in this study are available on request from the corresponding author.

Conflicts of Interest: The authors declare no conflict of interest.

References

1. Bai, Z.; Zhang, Q.; Zhang, Y.; Huang, Z.; Gao, Y.; Liu, J.; Wang, X. Enhanced photocurrent of self-powered ultraviolet photodetectors based on Ba1-xSrxTiO3 ceramics via ferroelectric polarization. *J. Alloy. Compd.* **2021**, *885*, 161177. [CrossRef]
2. Ariga, K. Nanoarchitectonics: What's coming next after nanotechnology? *Nanoscale Horiz.* **2021**, *6*, 364–378. [CrossRef]
3. Nam, C.-Y.; Jaroenapibal, P.; Tham, D.; Luzzi, D.E.; Evoy, S.; Fischer, J.E. Diameter-dependent electromechanical properties of GaN nanowires. *Nano Lett.* **2006**, *6*, 153–158. [CrossRef] [PubMed]
4. Huang, H.; Qian, Z.; Yang, J. IV characteristics of a piezoelectric semiconductor nanofiber under local tensile/compressive stress. *J. Appl. Phys.* **2019**, *126*, 164902. [CrossRef]
5. Guo, M.; Lu, C.; Qin, G.; Zhao, M. Temperature gradient-dominated electrical behaviours in a piezoelectric PN junction. *J. Electron. Mater.* **2021**, *50*, 947–953. [CrossRef]
6. Lu, S.; Qi, J.; Liu, S.; Zhang, Z.; Wang, Z.; Lin, P.; Liao, Q.; Liang, Q.; Zhang, Y. Piezotronic interface engineering on ZnO/Au-based Schottky junction for enhanced photoresponse of a flexible self-powered UV detector. *ACS Appl. Mater. Interfaces* **2014**, *6*, 14116–14122. [CrossRef] [PubMed]
7. Yang, M.; Zhang, X.; Ozkan, C.S. Modeling and optimal design of high-sensitivity piezoresistive microcantilevers within flow channels for biosensing applications. *Biomed. Microdevices* **2003**, *5*, 323–332. [CrossRef]

8. Wu, J.M.; Chen, K.-H.; Zhang, Y.; Wang, Z.L. A self-powered piezotronic strain sensor based on single $ZnSnO_3$ microbelts. *RSC Adv.* **2013**, *3*, 25184–25189. [CrossRef]
9. Mai, W.; Liang, Z.; Zhang, L.; Yu, X.; Liu, P.; Zhu, H.; Cai, X.; Tan, S. Strain sensing mechanism of the fabricated ZnO nanowire-polymer composite strain sensors. *Chem. Phys. Lett.* **2012**, *538*, 99–101. [CrossRef]
10. Peng, L.; Hu, L.; Fang, X. Energy harvesting for nanostructured self-powered photodetectors. *Adv. Funct. Mater.* **2014**, *24*, 2591–2610. [CrossRef]
11. Lin, P.; Yan, X.; Zhang, Z.; Shen, Y.; Zhao, Y.; Bai, Z.; Zhang, Y. Self-powered UV photosensor based on PEDOT:PSS/ZnO micro/nanowire with strain-modulated photoresponse. *ACS Appl. Mater.* **2013**, *5*, 3671–3676. [CrossRef] [PubMed]
12. Lin, P.; Yan, X.; Liu, Y.; Li, P.; Lu, S.; Zhang, Y. A tunable ZnO/electrolyte heterojunction for a self-powered photodetector. *Phys. Chem. Chem. Phys.* **2014**, *16*, 26697–26700. [CrossRef] [PubMed]
13. Luo, Q.; Tong, L. Constitutive modeling of photostrictive materials and design optimization of microcantilevers. *J. Intell. Mater. Syst. Struct.* **2009**, *20*, 1425–1438. [CrossRef]
14. Grundmann, M. *The Physics of Semiconductors*; Springer: Berlin/Heidelberg, Germany, 2010.
15. Wang, Z.L. Progress in Piezotronics and Piezo-Phototronics. *Adv. Mater.* **2012**, *24*, 4632–4646. [CrossRef]
16. Zhang, W.; Jiang, D.; Zhao, M.; Duan, Y.; Zhou, X.; Yang, X.; Shan, C.; Qin, J.; Gao, S.; Liang, Q.; et al. Piezo-phototronic effect for enhanced sensitivity and response range of ZnO thin film flexible UV photodetectors. *J. Appl. Phys.* **2019**, *125*, 024502. [CrossRef]
17. Wallys, J.; Hoffmann, S.; Furtmayr, F.; Teubert, J.; Eickhoff, M. Electrochemical properties of GaN nanowire electrodes-Influence of doping and control by external bias. *Nanotechnology* **2012**, *23*, 165701. [CrossRef]
18. Gao, P.; Wang, Z.Z.; Liu, K.H.; Xu, Z.; Wang, W.L.; Bai, X.D.; Wang, E.G. Photoconducting response on bending of individual ZnO nanowires. *J. Mater. Chem.* **2009**, *19*, 1002–1005. [CrossRef]
19. Guo, W.; Yang, Y.; Qi, J.; Zhao, J.; Zhang, Y. Localized ultraviolet photoresponse in single bent ZnO micro/nanowires. *Appl. Phys. Lett.* **2010**, *97*, 133112. [CrossRef]
20. Yu, J.; Huang, B.; Zheng, X.; Wang, H.; Chen, F.; Xie, S.; Wang, Q.; Li, J. Spatiotemporally correlated imaging of interfacial defects and photocurrents in high efficiency triple-cation mixed-halide perovskites. *Small* **2022**, *18*, 2200523. [CrossRef]
21. Li, Y.-H.; Yu, C.-B.; Li, Z.; Jiang, P.; Zhou, X.-Y.; Gao, C.-F.; Li, J. Layer-dependent and light-tunable surface potential of two-dimensional indium selenide (InSe) flakes. *Rare Metals* **2020**, *39*, 1356–1363. [CrossRef]
22. Hu, Y.; Chang, Y.; Fei, P.; Snyder, R.L.; Wang, Z.L. Designing the Electric Transport Characteristics of ZnO Micro/Nanowire Devices by Coupling Piezoelectric and Photoexcitation Effects. *ACS Nano* **2010**, *4*, 1234–1240. [CrossRef] [PubMed]
23. Wang, Z.; Qi, J.; Lu, S.; Li, P.; Li, X.; Zhang, Y. Enhancing sensitivity of force sensor based on a ZnO tetrapod by piezo-phototronic effect. *Appl. Phys. Lett.* **2013**, *103*, 143125. [CrossRef]
24. Lin, P.; Gu, Y.S.; Yan, X.Q.; Lu, S.N.; Zhang, Z.; Zhang, Y. Illumination-dependent free carrier screening effect on the performance evolution of ZnO piezotronic strain sensor. *Nano Res.* **2016**, *9*, 1091–1100. [CrossRef]
25. Huang, J.H.; Wang, X.J.; Wang, J. A mathematical model for predicting photo-induced voltage and photostriction of PLZT with coupled multi-physics fields and its application. *Smart Mater. Struct.* **2015**, *25*, 025002. [CrossRef]
26. Zhao, M.; Wang, Y.; Guo, C.; Lu, C.; Xu, G.; Qin, G. Temperature-dependent bending strength in piezoelectric semiconductive ceramics. *Ceram. Int.* **2021**, *48*, 2771–2775. [CrossRef]
27. Zhao, M.; Pan, Y.; Fan, C.; Xu, G. Extended displacement discontinuity method for analysis of cracks in 2D thermal piezoelectric semiconductors. *Smart Mater. Struct.* **2017**, *26*, 085029. [CrossRef]
28. Fan, C.Y.; Yan, Y.; Xu, G.T.; Zhao, M.H. Piezoelectric-conductor iterative method for analysis of cracks in piezoelectric semiconductors via the finite element method. *Eng. Fract. Mech.* **2016**, *165*, 183–196. [CrossRef]
29. Vasileska, D.; Goodnick, S.M.; Klimeck, G. *Computational Electronics: Semiclassical and Quantum Device Modeling and Simulation*; CRC Press: Boca Raton, FL, USA, 2017.
30. Cheng, R.; Zhang, C.; Yang, J. Thermally induced carrier distribution in a piezoelectric semiconductor fiber. *J. Electron. Mater.* **2019**, *48*, 4939–4946. [CrossRef]
31. Dai, X.; Zhu, F.; Qian, Z.; Yang, J. Electric potential and carrier distribution in a piezoelectric semiconductor nanowire in time-harmonic bending vibration. *Nano Energy* **2018**, *43*, 22–28. [CrossRef]
32. Holzapfel, G.A. Nonlinear solid mechanics: A continuum approach for engineering science. *Meccanica* **2002**, *37*, 489–490. [CrossRef]
33. Bykhovski, A.; Gelmont, B.; Shur, M.; Khan, A. Current-voltage characteristics of strained piezoelectric structures. *J. Appl. Phys.* **1995**, *77*, 1616–1620. [CrossRef]
34. Araneo, R.; Bini, F.; Pea, M.; Notargiacomo, A.; Rinaldi, A.; Lovat, G.; Celozzi, S. Current–voltage characteristics of ZnO nanowires under uniaxial loading. *IEEE Trans. Nanotechnol.* **2014**, *13*, 724–735. [CrossRef]
35. Sze, S.M.; Li, Y.; Ng, K.K. *Physics of Semiconductor Devices*; John Wiley & Sons: Hoboken, NJ, USA, 2021.
36. Qin, G.S.; Ma, S.J.; Lu, C.S.; Wang, G.; Zhao, M.H. Influence of electric field and current on the strength of depoled GaN piezoelectric semiconductive ceramics. *Ceram. Int.* **2018**, *44*, 4169–4175. [CrossRef]
37. Qin, G.S.; Zhou, X.P.; Wang, Y.; Lu, C.S.; Zhao, M.H. Polarization-dominated thermal-electric-mechanical behaviours in GaN ceramics. *Ceram. Int.* **2022**, *48*, 29816–29821. [CrossRef]
38. Levinshtein, M.E.; Rumyantsev, S.L.; Shur, M.S. *Properties of Advanced Semiconductor Materials: GaN, AIN, InN, BN, SiC, SiGe*; John Wiley & Sons: Hoboken, NJ, USA, 2001.

39. Jayaprakash, R.; Ajagunna, D.; Germanis, S.; Androulidaki, M.; Tsagaraki, K.; Georgakilas, A.; Pelekanos, N.T. Extraction of absorption coefficients from as-grown GaN nanowires on opaque substrates using all-optical method. *Opt. Express* **2014**, *22*, 19555–19566. [CrossRef]
40. Kremer, R.K.; Cardona, M.; Schmitt, E.; Blumm, J.; Estreicher, S.K.; Sanati, M.; Bockowski, M.; Grzegory, I.; Suski, T.; Jezowski, A. Heat capacity of $\alpha-$GaN: Isotope effects. *Phys. Rev. B* **2005**, *72*, 075209. [CrossRef]
41. Guo, M.K.; Qin, G.S.; Lu, C.; Zhao, M.H. Nonlinear solution of a piezoelectric PN junction under temperature gradient. *Int. J. Appl. Mech.* **2022**, *14*, 2150125. [CrossRef]
42. Cheng, R.; Zhang, C.; Chen, W.; Yang, J. Temperature effects on PN junctions in piezoelectric semiconductor fibers with thermoelastic and pyroelectric couplings. *J. Electron. Mater.* **2020**, *49*, 3140–3148. [CrossRef]
43. Araneo, R.; Lovat, G.; Falconi, C.; Notargiacomo, A.; Rinaldi, A. Accurate models for the current-voltage characteristics of vertically compressed piezo-semiconductive quasi-1D NWs. *MRS Online Proc. Libr.* **2013**, *1556*, 803. [CrossRef]
44. Colinge, J.P.; Colinge, C.A. *Physics of Semiconductor Devices*; Springer: New York, NY, USA, 2005.
45. Khusayfan, N.M.; Qasrawi, A.F.; Khanfar, H.K. Impact of Yb, In, Ag and Au thin film substrates on the crystalline nature, Schottky barrier formation and microwave trapping properties of Bi_2O_3 films. *Mater. Sci. Semicond. Process.* **2017**, *64*, 63–70. [CrossRef]
46. Zhou, L. Development and Characterization of Ohmic and Schottky Contacts for Gallium N and Aluminum Gallium Nitride Devices. Ph.D. Thesis, University of Illinois at Urbana-Champaign, Champaign, IL, USA, 2002.
47. Guo, P.; Jiang, J.; Shen, S.; Guo, L. ZnS/ZnO heterojunction as photoelectrode: Type II band alignment towards enhanced photoelectrochemical performance. *Int. J. Hydrog. Energy* **2013**, *38*, 13097–13103. [CrossRef]
48. Lin, P.; Chen, X.; Yan, X.; Zhang, Z.; Yuan, H.; Li, P.; Zhao, Y.; Zhang, Y. Enhanced photoresponse of Cu_2O/ZnO heterojunction with piezo-modulated interface engineering. *Nano Res.* **2014**, *7*, 860–868. [CrossRef]